Isothermal Growth and Reorganization upon Heating of a Single Poly(aryl−ether−ether−ketone) (PEEK) Spherulite, As Imaged by Atomic Force Microscopy

D. A. Ivanov[†] and A. M. Jonas*

Unité de Physique et de Chimie des Hauts Polymères, Université Catholique de Louvain, Place Croix du Sud 1, B-1348 Louvain-la-Neuve, Belgium (E.U.)

Received October 21, 1996

ABSTRACT: We have studied by atomic force microscopy (AFM, topographical imaging) the evolution of a single PEEK spherulite in a thin film during isothermal cold-crystallization and upon subsequent reheating to increasingly higher temperatures. To open the spherulitic microstructure, we added 30% w/w of an amorphous diluent (poly(ether−imide), PEI) serving as a marker. Small-angle X-ray scattering and dynamic mechanical analysis were used to check on bulk samples that similar structural evolutions are obtained when reheating cold-crystallized PEEK and a 70/30 PEEK/PEI blend. We then monitored at $T_c = 180$ °C the isothermal growth of a single PEEK spherulite in a thin film of the PEEK/PEI blend and followed the growth and branching of individual PEEK fibrils, separated by channels of rejected PEI. Further, we examined the changes in semicrystalline morphology induced by subsequent reheating. The spatial locations of the fibrils (i.e., lamellar stacks) of this very spherulite were not modified up to an annealing temperature of about 300 °C. However, the surface of the fibrils became covered with numerous small protuberances (diameter: 50−200 nm) growing in size and in number as annealing temperature increased. We consider these images to be the first direct-space proof for the existence of a large-scale melting−recrystallization process occurring when reheating cold-crystallized PEEK.

Introduction

The solid-state properties of a semicrystalline polymer are complex functions of its thermal history. The complexity of this dependence partially results from the out-of-equilibrium, or metastable character, of semicrystalline structures.[1] This metastability can be revealed in very simple experiments with heating−cooling cycles, performed below the main melting region of the polymer. The changes in some structural parameters induced by this thermal cycling can be classified with respect to their reversibility. The frequently observed irreversible behavior of these parameters clearly indicates the metastability of the structure.

In the case of PEEK (poly(oxy-1,4-phenyleneoxy-1,4-phenylenecarbonyl-1,4-phenylene)), a typical aromatic semicrystalline polymer, a large variation of structural parameters with crystallization (T_c) or annealing temperature is well-documented.[2−5] In a recent examination of the microstructural evolution of cold-crystallized PEEK during heating−cooling cycles,[6] it has been shown that large irreversible morphological variations can be induced in the sample when the annealing temperature exceeds the highest annealing temperature in the sample previous thermal history (T_{cmax}). These irreversible variations were detected in a temperature range well below the main melting endotherm observed in differential scanning calorimetry (DSC) experiments (∼350 °C). By contrast, only reversible variations were observed when heating and cooling the PEEK sample below its T_{cmax}. The irreversible morphological changes indicate that the perturbation applied to the metastable system by the temperature increase is sufficiently strong to transfer the system to another state of lower free energy in the time scale of the experiment. We denoted this mechanism as "melting−recrystallization" in accordance with other previous works in the field.[7−9] Associated with this melting−recrystallization, a double melting behavior is frequently observed for cold-crystallized PEEK. While the attribution of this double melting to the melting−recrystallization mechanism has been opposed by a few authors,[10−12] the existence of melting−recrystallization processes during the reheating of cold-crystallized PEEK samples is agreed upon by many workers in the field,[6,13,14] based on detailed analysis of thermal behavior (DSC) or X-ray scattering. Ideally, these conclusions would require support from independent direct-space observations. There have been a number of optical and electron microscopy studies performed on the PEEK morphology.[2,11,15−20] However, to the best of our knowledge, direct-space evidence for the existence of melting−recrystallization processes have not been conclusively obtained so far. It is the purpose of the present work to perform the first direct-space observations of the recrystallization processes occurring when reheating cold-crystallized PEEK samples.

For this purpose, we used atomic force microscopy (AFM) in the topographic mode to achieve a demanding task, i.e., the repetitive imaging of single elements of the semicrystalline structure in the course of their evolution [an abstract of this work was published in ref 21]. The choice of the recently developed AFM technique is advantageous as compared to optical, transmission electron, or scanning electron microscopies. First, the resolution of AFM may be on a par with that of electron microscopy in favorable instances.[22,23] Compared to optical polarizing microscopy, AFM does not give direct information about the crystallographic orientations. However, the resolution limits of optical techniques often prevent a detailed visualization of

[†] Present address: Laboratoire de Physique des Polymères, CP 223, Université libre de Bruxelles, Boulevard du Triomphe, 1050 Bruxelles, Belgium.

S0024-9297(96)01549-5 CCC: $15.00
Published on Web 06/18/1998

submicron spherulitic features.[24] Second, AFM represents a nondestructive type of analysis and does not require irreversible sample preparation (etching or sputtering of metal or carbon on the surface). Thus AFM does not preclude a repetitive assessment of the same intact polymer surface throughout different thermal treatments, which is crucial for studying reorganization processes.

Experimental Section

Thin Films. The PEEK powder (ICI, grade 150P) was dried overnight at 80 °C under vacuum. It was dissolved in benzophenone near its boiling point (305 °C) under a nitrogen atmosphere for 10−15 min at concentrations of about 0.1% and cast on freshly cleaved mica. The films were annealed for 10 min at 400 °C in order to evaporate the solvent and melt the polymer. Subsequent quenching to room temperature (RT) was performed by quickly sliding the mica substrate from the hot plate onto a metallic surface at RT. No traces of semicrystalline structure could be detected in the quenched films by AFM (resolution level of 10 nm). Continuous featureless films with flat surfaces of several angstroms roughness and thicknesses in the range 20−200 nm were obtained. Experiments on PEEK/poly(ether−imide) (PEI) films were also performed. The same procedure as described above was used, with some PEI (Ultem 1000, GE) added to PEEK by solution blending in benzophenone. The crystallization of PEEK and the 70/30 PEEK/PEI blend was performed from the glass at $T_{c,init}$'s of 156 and 180 °C, respectively (i.e. 13 and 19 °C above the corresponding T_g of the pure amorphous materials).

AFM topography images were recorded in contact mode (constant force) on our thin films with an Autoprobe CP (Park Scientific Instruments, Sunnyvale, CA). For some experiments, a special procedure was devised in order to monitor the evolution of single elements of the semicrystalline structure throughout different thermal treatments. Due to the fact that thermal treatments were not carried out in situ, it was necessary each time to find back the initial position and orientation of the specimen with respect to the scanner. For this purpose special copper grids for electron microscopy (Laborimpex) with labeled 40 × 40 μm cells were used. The grids were glued on the lower side of the mica substrate with a temperature-resistant epoxy-based thermosetting resin (Ciba). The grids strongly facilitated the repetitive search of the same area of the samples with a reflection optical microscope installed inside the AFM. The final refinement of position of an analyzed area was performed in AFM mode using as references the coordinates of the centers of a few spherulites, inside the grid-delimited area. Between two successive AFM observations, the samples were placed into the DMA oven in order to continue the isothermal crystallization of the sample or to reheat them to progressively larger temperatures (T_{cmax}) at a rate of 1.0 °C/min.

Bulk Samples. Quenched amorphous PEEK bulk sheets (350−500 μm thick) were prepared as described elsewhere.[6] Amorphous sheets of 70/30 PEEK/PEI blend of the same thickness were prepared by solution blending. After the solvent (benzophenone) was washed out with acetone in a Soxhlet apparatus for 48 h and the powder subsequently dried, the blend was compression-molded and quenched in accordance with ref 27. Some of these samples were isothermally crystallized at $T_{c,init}$ = 156 or 180 °C for PEEK and 70/30 PEEK/PEI, respectively. Others were initially crystallized for about 180 min at $T_{c,init}$ = 153 °C (PEEK) and 180 °C (70/30 PEEK/PEI) and reheated stepwise at 1.0 °C/min up to selected temperatures (T_{cmax}) between the initial $T_{c,init}$'s and 305 °C. The initial isothermal crystallization (before reheating of the samples) was sufficiently long to provide completely space-filling spherulites.

Small-angle X-ray scattering (SAXS) experiments were performed on these bulk samples in an evacuated compact Kratky camera mounted on a Siemens rotating anode generator (Ni-filtered Cu Kα radiation, 40 kV/300 mA). A position sensitive proportional counter (PSPC, Braun) was used to record the diffraction patterns. The data were first corrected for absorption, parasitic scattering, and detector dead time. After subtraction of the fluidlike scattering represented by Ruland's approximation,[25] the data were desmeared using a variant of Glatter's algorithm.[26] The long period (L_B) was taken as the distance corresponding to the maximum of the Lorentz-corrected desmeared scattering.

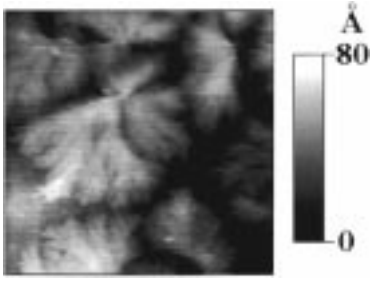

Figure 1. Room temperature 5.0 μm × 5.0 μm AFM topographic image of a PEEK thin film isothermally crystallized for 15 min at 156 °C. The full gray scale corresponds to 80 Å.

Dynamic mechanical analysis (DMA) was performed in tension mode in a Rheometrics RSA II on rectangular 5 × 30 mm^2 bulk specimens (test frequency, 1 Hz; dynamic deformation, 0.02%). The glass transition temperature T_g was defined as the temperature corresponding to the maximum of the dynamic mechanical loss modulus.

Results and Discussion

Although the observation of pure PEEK spherulites in thin solution cast films proved to be possible by AFM, the resolution of the technique was however insufficient to disclose internal subspherulitic details, and the overall quality of the images obtained needed to be improved (Figure 1). In addition, only vague and indistinct images could be obtained after reheating the samples to temperatures larger than their $T_{c,init}$. While this suggested that the sample surface reorganized during the subsequent heating, it was not possible to obtain further meaningful information.

Hence, to obtain a spherulitic morphology more amenable to discussion, we added an amorphous diluent (PEI) to the system. PEI is known to be fully miscible with PEEK in the amorphous state over the entire composition range.[28] Moreover, PEI segregates largely in the interfibrillar regions upon PEEK crystallization, with little disturbance of the interlamellar amorphous regions.[27,28] Thus, the presence of PEI is not expected to change significantly the properties of semicrystalline PEEK at the lamellar scale, in accordance with results of optical and electron microscopy studies on PEEK/PEI blends.[29,30] Synchrotron studies of the structural evolution of PEEK/PEI during heating−cooling cycles[6] suggested an essentially identical behavior of pure PEEK and PEEK/PEI blends at the lamellar scale. Thus, one might assume that PEI can be simply considered as a marker, which will help us to separate better the PEEK fibrils in spherulites and to facilitate the spatial resolution of reorganization processes.

To be more positive about this issue, we have compared the structural evolutions of bulk PEEK and PEEK/PEI samples cold-crystallized near their respective T_g's and then annealed to increasing temperatures. The main results are presented in Figures 2 and 3. Figure 2a,b displays the evolution of T_g and long period (L_B) as a function of crystallization time (left) or annealing temperature (right), while Figure 3 shows the

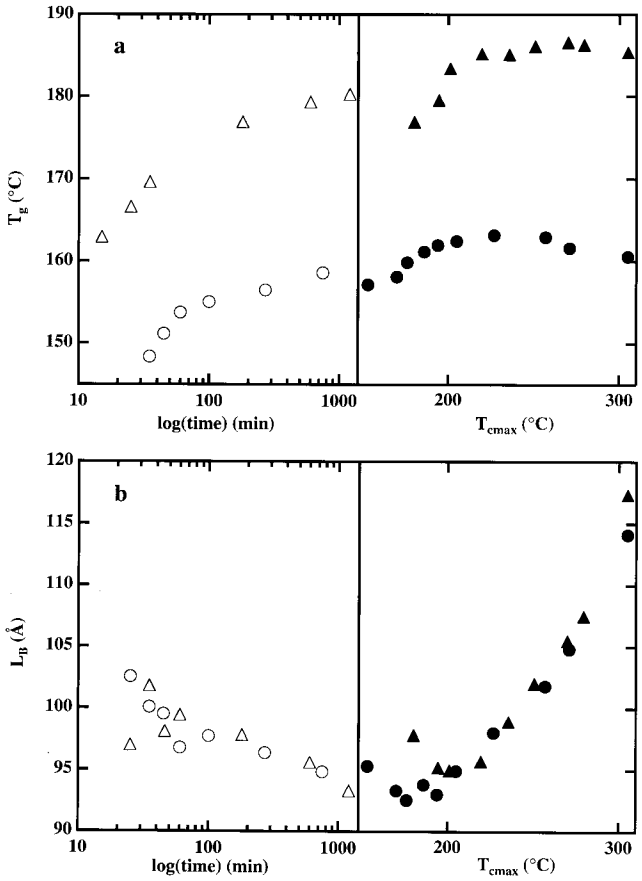

Figure 2. (a) Evolution of the glass transition temperature of amorphous interlamellar regions (left) with crystallization time at 156 °C (PEEK) or 180 °C (70/30 PEEK/PEI) and (right) with temperature upon subsequent reheating after 3 h of isothermal crystallization at 153 °C (PEEK) and 180 °C (70/30 PEEK/PEI). Symbols: ○, ●, PEEK; △, ▲, 70/30 PEEK/PEI. (b) Evolution of the SAXS long period with crystallization time at 156 °C (PEEK: ○) or 180 °C (70/30 PEEK/PEI: △) and with temperature upon subsequent reheating after 3 h of isothermal crystallization at 153 °C (PEEK: ●) and 180 °C (70/30 PEEK/PEI: ▲).

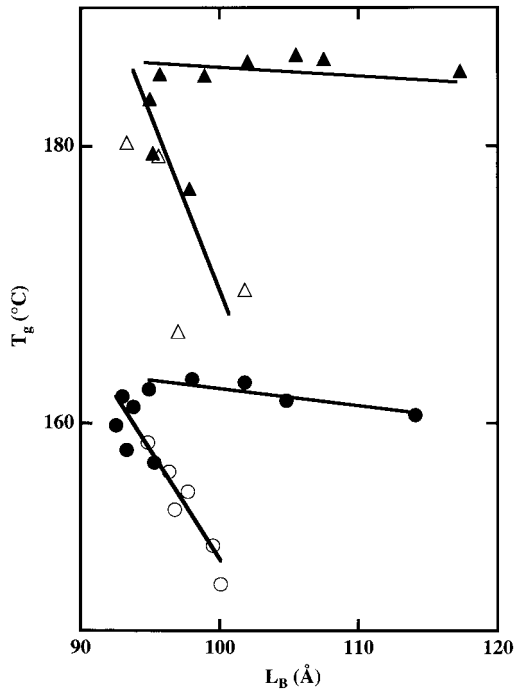

Figure 3. Glass transition temperature of amorphous interlamellar regions versus SAXS long period. The presence of two regimes of reorganization is readily apparent on this graph, as well as the essentially identical behavior of PEEK (○, ●) and 70/30 PEEK/PEI (△, ▲) (open symbols, isothermal crystallization; filled symbols, reheating). The first regime (steeper branches) corresponds to crystallization or annealing at low temperatures. A large variation of T_g accompanied by a slight decrease of long period is observed. The mechanisms occurring in this first regime are complex, with vitrification/devitrification of amorphous regions playing an important role.[31] The second regime (less steep branches) corresponds to annealing at higher temperatures. Significant increase of long period and a slight decrease of T_g can be detected in this regime. The morphological changes in this regime reflect large-scale melting−recrystallization processes.

corresponding plot of T_g versus L_B. From these graphs, the existence of two regimes of reorganization is readily apparent.

In the low annealing temperature range (T_{cmax} below 220−240 °C), the first regime manifests itself by large variations of T_g with a small decrease of long period, as crystallization time or annealing temperature increase. This regime occurs for T_{cmax}'s corresponding to the range of the broad loss modulus of the PEEK α-relaxation (associated with its glass transition). The mechanisms occurring in this first regime are complex, with vitrification/devitrification of amorphous regions during crystallization/annealing playing an important role.[31]

The second regime is characterized by a large increase of L_B as T_{cmax} increases, with a relatively limited decrease of T_g. In this second regime, the melting−recrystallization of the samples annealed at increasingly higher temperature gives rise to lamellar structures with increasingly large crystals and amorphous intercrystalline regions. The larger size of the amorphous interlayers allows for a decrease of the average constraints experienced by amorphous regions due to their connection to nearby crystals, resulting in a decrease of glass transition temperature.[3,32] This is the region we are essentially concerned with in this paper. From Figure 2, it is obvious that PEEK and the 70/30 PEEK/PEI blend behave similarly, with the obvious difference that the glass transition temperatures of the interlamellar regions of the blend are somewhat higher than those of pure PEEK, due to partial incorporation of PEI into these regions.[27] Hence, we may safely conclude that the examination of the microstructural evolution of PEEK/PEI blends with T_{cmax} will bring information relevant to the case of pure PEEK as well.

Figure 4a−d presents the evolution of a single PEEK spherulite from a 70/30 PEEK/PEI blend, during its isothermal growth at $T_{c,init} = 180$ °C. The subspherulitic resolution allows one to visualize the growth and branching of individual fibrils (i.e. stacks of lamellae) separated by channels of rejected PEI. The estimated characteristic length scale of segregation amounts in our case to 0.2−0.3 μm. No significant amount of interspherulitic segregation is evidenced. As soon as the fibrillar tips of adjacent spherulites come into contact, further growth is stopped with little if any spherulitic interpenetration. The almost linear interspherulitic boundary visible in the upper left part of the images indicates the constancy of the outward growth rate up to the moment of impingement. The growth rate evaluated for several individual fibrils is about 0.2−0.4 μm/min. The final shape of the spherulite is clearly reminiscent of the initial pattern of fibrils spreading out from the central nucleus.

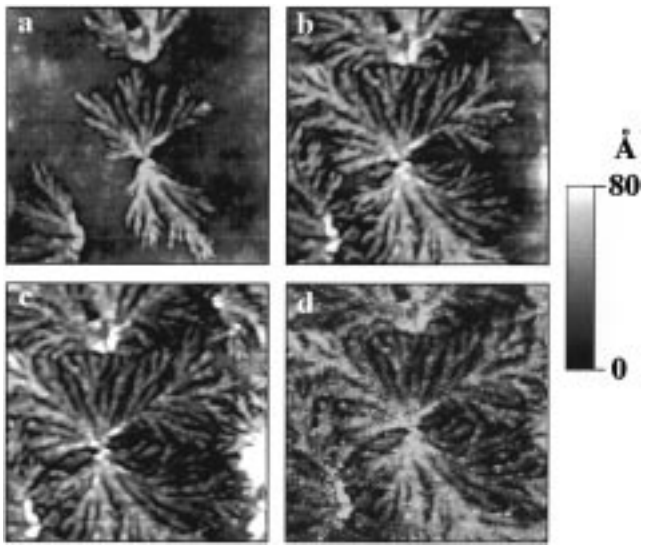

Figure 4. Room-temperature 5.0 μm × 5.0 μm AFM topographic images of a PEEK/PEI (70/30) thin film isothermally crystallized for different times (t_c) at 180 °C. The experiments are performed on a single spherulite repeatedly scanned after thermal treatment: (a) t_c = 4 min; (b) t_c = 8 min; (c) t_c = 12 min; (d) t_c = 60 min. The full gray scale is identical for all images and corresponds to 80 Å.

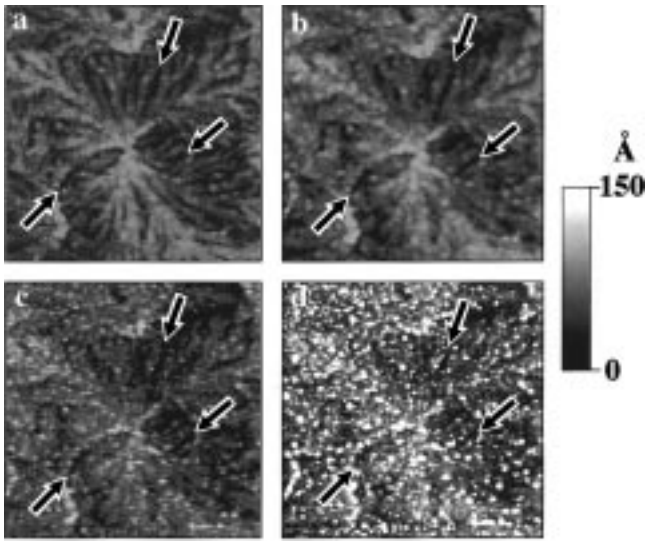

Figure 5. Room-temperature 5.0 μm × 5.0 μm AFM topographic images of a PEEK/PEI (70/30) thin film isothermally crystallized for 1 h at 180 °C (a) and then slowly reheated to higher T_{cmax}'s at 1 °C/min. The observed spherulite is the very same spherulite that was repeatedly imaged during isothermal crystallization (Figure 4a−d): (b) T_{cmax} = 220 °C; (c) T_{cmax} = 260 °C; (d) T_{cmax} = 300 °C. The full gray scale is identical for all images and corresponds to 150 Å. This value was chosen to reveal the changes in semicrystalline morphology occurring upon reheating of cold crystallized film (see details in the text). As a consequence, the main features of the underlying spherulite appear less contrasted than in Figure 4. To help the reader, arrows indicate on each photograph the location of identical PEI channels.

The result of the progressive reheating of this spherulite up to T_{cmax} = 300 °C is presented in Figure 5a−d. It is important to realize that the same very spherulite was imaged throughout and that the full gray scale is kept constant and equal to 150 Å for all images of Figure 5. This value was selected to reveal the changes in semicrystalline morphology occurring upon reheating of the cold-crystallized film. As a consequence, the main features of the underlying spherulite appear less contrasted than in Figure 4, where full gray scale corresponds to 80 Å. To help the reader, arrows indicate on each photograph the location of identical PEI channels.

Although the appearance of the spherulite is strongly affected by the annealing, the main features of the spherulite are still distinguishable. This is because the spatial locations of the fibrils, isolated by the interfibrillar PEI channels, remain fixed throughout the treatments. The PEI-rich regions essentially remain unaffected during the annealings, providing the frame which permits the repeated identification of the spherulite.

By contrast, the fibrils are strongly affected by the annealing, to the point that the general appearance of the spherulites is much disturbed. These changes apparently consist in the formation of numerous small protuberances growing in number and in size as T_{cmax} increases. The appearance of these protuberances does not result from damages that would have been created by the AFM tip while rastering in a scan and magnified for some reason during the next reheating. Indeed, the same morphology is observed at other locations on the same specimen, irrespective of the fact that they were or not previously imaged by AFM.

We view the dramatic evolution displayed in Figure 5 as the direct-space manifestation of the melting−recrystallization mechanisms already postulated by less direct techniques such as DSC and SAXS. Indeed, the size of the new morphological features (protuberances) strongly suggests the occurrence of large-scale motions of the PEEK chains during reheating, extending over distances significantly larger than the long period of the semicrystalline structure as determined by SAXS. This is only possible provided substantial melting of the PEEK crystals occurs inside lamellar stacks during heating ramps. Moreover, the extent of the observed microstructural changes (amount of protuberances) is not compatible with them being associated with the melting of a minority of crystals. In addition, the detected increase of the long period in this annealing regime is only possible provided a series of neighboring crystals melt and recrystallize into a fully reorganized stack. Hence, from the size and amount of the protuberances formed during reheating, and the additional information provided by SAXS, one can safely conclude that a melting−recrystallization process is operating during the annealing experiments.

Conclusion

Taking advantage of the nondestructive character of the AFM technique, we succeeded in performing the repetitive imaging of a single PEEK spherulite in thin film during its isothermal cold-crystallization and subsequent reheating to progressively increasing temperatures. This required however the addition of 30% of an amorphous diluent (PEI) in order to obtain a more open morphology allowing us to resolve subspherulitic features. We checked on bulk samples that similar structural evolutions are obtained upon annealing samples of pure PEEK and of 70/30 PEEK/PEI cold-crystallized near their respective glass transition temperatures. This ensures that the observations performed on the blends are applicable to pure PEEK as well.

Morphological observations during isothermal crystallization indicate the constancy of the growth rate up to the moment of impingement and the absence of any significant interspherulitic segregation. Reheating the

spherulite to increasingly higher T_{cmax} results in the appearance of numerous protuberances on the spherulite's fibrils. This effect is much more pronounced for T_{cmax}'s above 220−240 °C, where SAXS indicates the existence of large-scale reorganization process in PEEK. Accordingly, we consider the appearance of these protuberances as the first direct-space proof for the existence of a melting−recrystallization process occurring upon reheating cold-crystallized PEEK samples. From the size and amount of these protuberances, one may infer that this mechanism concerns a majority of PEEK crystals, which is in good agreement with previous DSC and SAXS studies performed on cold-crystallized PEEK.

At this stage, it is appropriate to remark that extreme caution should be taken when attempting to construct a complete and consistent model for the semicrystalline structure of PEEK and other similar aromatic polymers. Indeed, the out-of-equilibrium nature of this structure makes it sensitive to details of its thermal history. Thus, it is for instance to be expected that samples crystallized from the melt in a stepwise manner[33] may behave quite differently from our cold-crystallized samples. This point has been discussed more extensively elsewhere.[6,13] Nevertheless, for cold-crystallized samples, the present study provides strong support to importance of melting−recrystallization effects on the microstructure of PEEK during its reheating above its initial crystallization temperature.

Acknowledgment. Partial financial support of this work by the Belgian National Fund for Scientific Research (FNRS) is gratefully acknowledged. We thank Prof. R. Legras for his permanent interest in our work and Dr. B. Nysten for many useful advice concerning the AFM experiments. We are indebted to Mr. A. Gijbels of Ciba-Geigy NV for the free delivery of a highly thermostable epoxide glue.

References and Notes

(1) Yagfarov, M. Sh. *Polym. Sci. U.S.S.R.* **1982**, *24*, 2915.
(2) Blundell, D. J.; Osborn, B. N. *Polymer* **1983**, *24*, 953.
(3) Jonas, A.; Legras, R. *Macromolecules* **1993**, *26*, 4489.
(4) Cebe, P. *J. Mater. Sci.* **1995**, *23*, 3721.
(5) Hay, J. N.; Langford, J. I.; Lloyd, J. R. *Polymer* **1989**, *30*, 4891.
(6) Jonas, A. M.; Russell, T. P.; Yoon, Do Y. *Macromolecules* **1995**, *28*, 8491.
(7) Lee, Y.; Porter, R. S. *Macromolecules* **1987**, *20*, 1336.
(8) Lee, Y.; Porter, R. S.; Lin, J. S. *Macromolecules* **1989**, *22*, 1756.
(9) Holdsworth, P. G.; Turner-Jones, A. *Polymer* **1971,** *12*, 195.
(10) Verma, R. K.; Hsiao, B. S. *Trends Polym. Sci.* **1996**, *4*, 312.
(11) Bassett, D. C.; Olley, R. H.; Al Raheil, I. A. M. *Polymer* **1988**, *29*, 1745.
(12) Cebe, P.; Hong, S. D. *Polymer* **1986**, *27*, 1183.
(13) Fougnies, C.; Damman, P.; Dosière, M.; Koch, M. H. J. *Macromolecules* **1997**, *30*, 1392.
(14) Blundell, D. J. *Polymer* **1987**, *28*, 2248.
(15) Lovinger, A. J.; Davis, D. D. *J. Appl. Phys.* **1985**, *58*, 2843.
(16) Lovinger, A. J.; Hudson, S. D.; Davis, D. D. *Macromolecules* **1992**, *25*, 1752.
(17) Kumar, S.; Anderson, D. P.; Adams, W. W. *Polymer* **1986**, *27*, 329.
(18) Marand, H.; Prasad, A. *Macromolecules* **1992**, *25*, 1731.
(19) Vaughan, A. S.; Stevens, G. C. *Polymer* **1995**, *36*, 1531.
(20) Lattimer, M. P.; Hobbs, J. K.; Hill, M. J.; Barham, P. J. *Polymer* **1992**, *33*, 3971.
(21) Ivanov, D. A.; Jonas, A. *Bull. Am. Phys. Soc.* **1996**, *41*, 395.
(22) Magonov, S. N. *Appl. Spectrosc. Rev.* **1993**, *28*, 1.
(23) Harron, H. R.; Pritchard, R. G.; Cope, B. C.; Goddard, D. T. *J. Polym. Sci., Part B: Polym. Phys.* **1996**, *34*, 173.
(24) Born, M.; Wolf, E. *Principles of optics*; Pergamon Press: Oxford, U.K., 1984.
(25) Wiegand, W.; Ruland, W. *Prog. Colloid Polym. Sci.* **1979**, *66*, 355.
(26) Glatter, O. *J. Appl. Crystallogr.* **1974**, *7*, 147.
(27) Jonas, A. M.; Ivanov, D. A.; Yoon, D. Y. Submitted for publication in *Macromolecules*.
(28) Crevecoeur, G.; Groeninckx, G. *Macromolecules* **1991**, *24*, 1190.
(29) Chen, H.-L.; Porter, R. S. *Polym. Eng. Sci.* **1992**, *32*, 1870.
(30) Hudson, S. D.; Davis, D. D.; Lovinger, A. J. *Macromolecules* **1992**, *25*, 5, 1759.
(31) Ivanov, D. A.; Jonas, A. M. *J. Polym. Sci., Part B: Polym. Phys.* **1998**, *36*, 919.
(32) Kalika, D. S.; Gibson, D. G.; Quiram, D. J.; Register, R. A. *J. Polym. Sci., Part B: Polym. Phys.* **1998**, *36*, 65.
(33) Krüger, K.-N.; Zachmann, H. G. *Macromolecules* **1993**, *26*, 5202.

MA961549E